Computers and Electronics in Agriculture 146 (2018) 93–103

Contents lists available at ScienceDirect

Computers and Electronics in Agriculture

journal homepage: www.elsevier.com/locate/compag

Original papers

Adaptive two time-scale receding horizon optimal control for greenhouse lettuce cultivation

Dan Xu[a,b], Shangfeng Du[a], Gerard van Willigenburg[b,*]

[a] China Agricultural University, Beijing 100083, PR China
[b] Mathematical and Statistical Methods Group (Biometris), Wageningen University, Droevendaalsesteeg 1, 6708 PB Wageningen, The Netherlands

ARTICLE INFO

Keywords:
Greenhouse cultivation
Adaptive control
Receding horizon optimal control
Time-scale decomposition

ABSTRACT

A two time-scale, receding horizon, optimal controller for greenhouse lettuce cultivation is extended with on-line parameter estimation to handle ill-known or time-varying parameters of the greenhouse-crop model. By means of simulations, the possible improvement of performance and reduction of constraint violation, introduced by this extension, are investigated. Moreover, uncommon issues in the adaptive controller design due to the two time-scales are considered and handled in this paper. The estimated parameters are selected based on their uncertainty and performance sensitivity. Using a recently developed very efficient algorithm, the selected parameters are checked for identifiability first. Finally the possibility of real-time implementation of the adaptive two time-scale receding horizon optimal controller is investigated.

1. Introduction

Greenhouses for crop cultivation provide shelter for crops to grow under unfavourable external weather. Also they enable growers to manipulate the greenhouse climate in order to increase quality and production (van Straten et al., 2010). Therefore the greenhouse industry is growing fast nowadays. In modern greenhouses, automatic control is replacing manual control. This cuts down the labour cost and increases management efficiency. However, the majority of these automatic controllers use set-points. These set-points are generally selected in a heuristic way based on rules of thumb and grower experience. These have resulted in a very large number (hundreds) of controller settings that are not transparent. Only some of these (roughly 10–20) are used by the grower while the rest remains at default values tuned or selected by the manufacturer. In practice, different growers often use different controller settings and associated values (van Straten et al., 2000).

As opposed to this, optimal control of greenhouse cultivation is a transparent, quantitative, model-based approach that is optimal in principle. This approach exploits scientific knowledge concerning greenhouses, crops and weather predictions to maximize profit. The scientific knowledge concerning greenhouses and crops is captured in a dynamic model. Profit is calculated from costs associated with greenhouse management, such as energy costs, as well as revenues obtained from selling crops. Knowledge of weather predictions and their uncertainty is used to estimate the model state on-line which in turn enables on-line optimal control. (van Straten, 2013).

Despite its favourable properties, optimal control of greenhouse cultivation still suffers from several problems. These relate to different time scales and rapidly fluctuating uncertain weather that acts as an external input (van Willigenburg et al., 2000). A major contribution in overcoming these problems, by means of time-scale decomposition and receding horizon optimal control, was made by van Henten (1994), see also van Henten and Bontsema (2009). Tap (2000) used and further developed this method for on-line implementation. A similar more recent contribution is by Gonzales et al. (2014). In this paper the method used by these authors is extended with on-line parameter estimation to investigate the possible improvement of performance and reduction of constraint violation. The estimated parameters are selected based on their uncertainties as well as the sensitivities of the controller performance (profit) to these parameters. Moreover the selection is guided by a recently developed very efficient algorithm that computes identifiability of to be estimated parameters for nonlinear systems. A different but related approach to determine such parameters is presented by Ioslovich (2004).

Past research reveals the importance of estimating uncertain model parameters on-line in greenhouse cultivation. Udink ten Cate and van de Vooren (1978), Udink ten Cate (1983), Davis (1984) and Hooper and Davis (1985) proposed and investigated adaptive control of greenhouse temperature through heating and ventilation based on a simplified model and PID control. Berenguel (2003) studied mixed feed-forward adaptive control. Arvanitis et al. (2000) proposed a scheme of multirate

* Corresponding author.
E-mail address: gerard.vanwilligenburg@wur.nl (G. van Willigenburg).

https://doi.org/10.1016/j.compag.2018.02.001
Received 25 August 2017; Received in revised form 29 January 2018; Accepted 1 February 2018

adaptive temperature control between pole-placement and linear quadratic regulation. Cunha (2006) realized real-time adaptive control for greenhouse heating, cooling and CO_2 enrichment. Rodríguez (2008) put forward a strategy of adaptive hierarchical control to keep humidity in a specific range through adapting temperature set-points. Speetjens (2008) and Speetjens et al. (2009) implemented an extended Kalman filter for on-line estimating model parameters to control the so called Watergy greenhouse.

To the best of our knowledge adaptive receding horizon optimal control incorporating a two time-scale decomposition has never been considered for greenhouse cultivation. Starting from a two time-scale receding horizon optimal controller this paper investigates improvement of control performance and reduction of state constraint violation achieved by adding on-line parameter estimation to this controller. The computational effort required by the adaptive two time-scale receding horizon optimal controller is also investigated to judge the possibility of real-time implementation on a personal computer.

2. Materials and methods

2.1. Greenhouse-crop model

Given our research goals stated in the introduction, and the fact that even well-established crop models and physical models of the greenhouse lack high accuracy (Ioslovich et al., 2009), for both we prefer a relatively small white box model. Such a greenhouse-crop model was presented by van Henten (2003). This model captures the main features of the greenhouse, crop and economics to enable on-line adaptive optimal control. Moreover, to allow for a proper understanding and interpretation, a white box model is preferred.

To further motivate our model choice several candidate models from the literature are discussed shortly. The greenhouse-crop model of Tap (2000) contains a so called 'big leaf, big fruit' reduced model of tomato, that described harvest throughout the season. We prefer a single harvest crop because it is more simple from an optimal control perspective.

Van Ooteghem (2007) models an advanced Dutch solar greenhouse. Compared to conventional Dutch greenhouses additional equipment is installed to promote energy efficiency. To model this equipment a significant number of additional states and smoothed switching functions are required, complicating the dynamics. Moreover this advanced greenhouse structure served a feasibility study. Up to now it is not used in practice.

The model used by van Beveren et al. (2015) is one for minimizing energy related to both heating and cooling of a greenhouse. It doesn't include a crop model because it takes greenhouse climate trajectories as an input. Also, cooling systems are still uncommon in greenhouses.

An interesting approach to greenhouse climate control is proposed by Ioslovich et al. (2009). They use a very large and well established tomato crop model (TOMGRO) while considering the greenhouse climate partly static. To enable optimal control they furthermore rely on a series of simplifying assumptions enabling partly analytical solutions of the optimal control problems. As opposed to this, one of our research goals is to investigate whether adaptive optimal control, including a time-scale decomposition, can be applied without making any simplifying assumptions. This is motivated by the fact that optimal control algorithms are increasingly well developed, user friendly and efficient (Tomlab, Rutquist and Edvall, 2010). They allow for on-line computations for processes that are not very fast, such as greenhouse climate (van Beveren et al., 2015).

The greenhouse-crop model of van Henten (2003), used in this paper, has three states being greenhouse temperature X_T, humidity X_h, and CO_2 concentration X_c The crop, being lettuce, has only one state being crop dry weight X_d. The lettuce crops are fully harvested at the end of the growing period. Constant parameters in the model are denoted by c with an associated subscript. U indicates a control variable, V an external weather variable while subscripts T, h, c, q, and v indicate respectively temperature, humidity, CO_2, heat, and ventilation. The differential equations representing the model are,

$$\frac{dX_d}{dt} = c_{\alpha\beta}\varphi_{phot,c} - c_{resp,d}X_d 2^{(0.1X_T-2.5)} \tag{1}$$

$$\frac{dX_c}{dt} = \frac{1}{c_{cap,c}}[-\varphi_{phot,c} + c_{resp,d}X_d 2^{(0.1X_T-2.5)} + U_c - \varphi_{vent,c}] \tag{2}$$

$$\frac{dX_T}{dt} = \frac{1}{c_{cap,q}}[U_q - Q_{vent,q} + Q_{rad,q}] \tag{3}$$

$$\frac{dX_h}{dt} = \frac{1}{c_{cap,h}}[\varphi_{transp,h} + \varphi_{vent,h}] \tag{4}$$

with,

$$\varphi_{phot,c} = (1-e^{-c_{pl,d}X_d})\frac{c_{rad,phot}V_{rad}(-c_{co_2,1}X_T^2 + c_{co_2,2}X_T - c_{co_2,3})(X_c - c_\Gamma)}{c_{rad,phot}V_{rad} + (-c_{co_2,1}X_T^2 + c_{co_2,2}X_T - c_{co_2,3})(X_c - c_\Gamma)} \tag{5}$$

$$\varphi_{vent,c} = (U_v + c_{leak})(X_c - V_c) \tag{6}$$

$$Q_{vent,q} = (c_{cap,q,v}U_v + c_{ai,ou})(X_T - V_T) \tag{7}$$

$$Q_{rad,q} = c_{rad,q}V_{rad} \tag{8}$$

$$\varphi_{transp,h} = (1-e^{c_{pl,d}X_d})c_{v,pl,ai}\left(\frac{c_{v,1}}{c_R(X_T + c_{T,abs})}e^{c_{v,2}X_T/(X_T+c_{v,3})} - X_h\right) \tag{9}$$

$$\varphi_{vent,h} = (U_c + c_{leak})(X_h - V_h) \tag{10}$$

As to the two time-scale decomposition, X_d is the slow state, while X_c, X_T, and X_h are fast states describing greenhouse climate. For further details, such as the subscripts of the constant model parameters and their corresponding values, and the physical meaning of variables, see van Henten (2003).

To apply the time-scale decomposition, a state-space representation of the model in which the fast and slow parts of the dynamics are distinguished, is convenient. To that end define the systems full state vector,

$$x = \begin{bmatrix} X_d \\ X_c \\ X_T \\ X_h \end{bmatrix} \tag{11}$$

the "slow state" vector corresponding to the slow dynamics,

$$x_s = X_d \tag{12}$$

and the "fast state" vector corresponding to the fast dynamics,

$$x_f = \begin{bmatrix} X_c \\ X_T \\ X_h \end{bmatrix} \tag{13}$$

the control input vector,

$$u = \begin{bmatrix} U_c \\ U_q \\ U_v \end{bmatrix} \tag{14}$$

and finally the vector of external inputs,

$$d = \begin{bmatrix} V_{rad} \\ V_T \\ V_c \\ V_h \end{bmatrix} \tag{15}$$

In state-space form the full system dynamics then read,

$$\frac{dx}{dt} = \begin{bmatrix} dX_d/dt \\ dX_c/dt \\ dX_T/dt \\ dX_h/dt \end{bmatrix} = f(x,u,d) \tag{16}$$

the “slow” dynamics read,

$$\frac{dx_s}{dt} = dX_d/dt = f_s(x,u,d) \tag{17}$$

and the “fast” dynamics,

$$\frac{dx_f}{dt} = \begin{bmatrix} dX_c/dt \\ dX_T/dt \\ dX_h/dt \end{bmatrix} = f_f(x,u,d) \tag{18}$$

2.2. Control objective and constraints

The economic performance measure is selected to be profit, which is maximized by the optimal control. The specification of profit P is also taken from van Henten (2003),

$$P = c_{pri,1} + c_{pri,2}X_d(t_f) - \int_{t_0}^{t_f} (c_q U_q(t) + c_{CO_2} U_c(t))dt \tag{19}$$

In Eq. (19) $c_{pri,1} + c_{pri,2}X_d(t_f)$ represents money obtained from selling all harvested crops $X_d(t_f)$. Since $c_{pri,1}$ is a constant, it does not affect the maximization but does influence the profit obtained by the grower. The expression $c_{pri,1} + c_{pri,2}X_d(t_f)$ results from an investigation into prices obtained for crops by different growers (van Henten, 2003). In Eq. (19) $c_q U_q(t) + c_{CO2} U_c(t)$ represents running costs associated with heating and CO_2 supply respectively. It is assumed that no costs are associated with ventilation (opening and closing windows).

In optimal control it is custom to minimize a cost function denoted by J. Maximization of profit (19) is equivalent to minimizing,

$$J = -P = -c_{pri,1} - c_{pri,2}X_d(t_f) + \int_{t_0}^{t_f} (c_q U_q(t) + c_{CO_2} U_c(t))dt \tag{20}$$

Because the crop model does not properly describe crop response to extreme values of temperature, humidity and CO_2 concentration these greenhouse state variables are upper and lower bounded. Van Henten (2003) uses penalty functions to penalize violations of these bounds. Penalty functions translate constraint violations into additional costs. This translation is difficult to design. Growers generally judge constraint violations very harmful and therefore want to totally prevent them. Since our optimal control software, described in Section 3.2, is capable of solving optimal control problems with both state and control constraints we decided to implement upper and lower bounds of state variables as constraints. Upper and lower bounds of greenhouse climate state variables are recorded in Table 1 where $X_{h,sat}$ is saturation water vapour pressure given by van Henten (2003),

$$X_{h,sat}(X_T) = \frac{c_{v,4}}{c_R(X_T + c_{T,abs})} e^{c_{v,2}X_T/(X_T + c_{v,3})} \tag{21}$$

2.3. Adaptive two time-scale receding horizon optimal controller

Time-scale decomposition within optimal control of greenhouse cultivation was introduced by van Henten (1994), see also van Henten and Bontsema (2009) and van Straten et al. (2010). Ordinary time-scale decomposition within optimal control is based on singular perturbation theory (Kokotović et al., 1986). In the case of greenhouse cultivation however, adjustments are required. This is caused by the weather acting as an external input that permanently excites the fast dynamics being the greenhouse climate. In conventional singular perturbation theory excitation of the fast dynamics only occurs very shortly just after the initial time and just before the final time.

In Fig. 1 a block diagram of the adaptive two time-scale receding horizon optimal controller is presented. Notice that, apart from the adaptive part of the controller represented by the two blocks at the bottom, the block diagram resembles the ones presented by van Henten (1994) and van Henten and Bontsema (2009). The greenhouse climate controller in the inner loop is a receding horizon optimal controller (RHOC) that uses the measured climate states as well as a short term weather prediction to on-line compute a new optimal control. The sampling time of this controller is in the order of 1–60 min while the horizon is in the order of a day. We selected a sampling period of 30 min and a control horizon of 3 h. This choice is a compromise that enables real-time implementation and also prevents introduction of a third time-scale (van Willigenburg, 2000). It may lead to state constraint violations but these will still be acceptable in practice since they do not last too long (in the order of 30 min).

The RHOC in the inner loop controls the fast dynamics of the greenhouse climate. It requires the state and co-state obtained from the optimal control computation in the outer loop. The co-state equals the marginal value of crop dry weight that determines partly the cost function used by the RHOC in the inner loop. The RHOC also counteracts errors such as erroneous short term weather predictions and modelling and measurement errors (van Henten, 2003; Gonzales et al., 2014). Errors or changes in the selling price of lettuce, represented by parameters $c_{pri,1}$ and $c_{pri,2}$ in Eqs. (19) and (20), as well as the price of heat energy and CO_2 are not counteracted by the RHOC. These can be taken into account by re-computing optimal controls in the outer loop of Fig. 1. These re-computations are based on maximization of profit that comes down to minimizing Eq. (20). They require dry weight measurement of the crop. If not available, the value computed from the model may be used. Dry weight measurements can be obtained by removing individual immature lettuce crops for measurement at several stages. Re-computation of the optimal control in the outer loop also allows for exploitation of improved long term weather predictions. The optimal control in the outer loop has to be computed at least once, before the actual control starts (van Henten, 1994; van Henten and Bontsema, 2009).

The optimal control computation in the outer loop uses a static approximation of the greenhouse climate dynamics obtained by setting to zero all associated state derivatives being $\frac{dX_c}{dt}$, $\frac{dX_T}{dt}$, and $\frac{dX_h}{dt}$ in Eqs. (2)–(4) respectively. This is acceptable because the long term weather predictions only represent slow weather variations not exciting the fast greenhouse dynamics. Next to the static approximation, the slow dynamic given by Eq. (1) are used to compute the optimal control in the outer loop. As to Fig. 1 one may state that the outer loop controls the slow dynamics while the inner loop controls the fast dynamics.

The adaptive part of the controller is represented by the lower two blocks estimating greenhouse and crop related parameters. The choice of these parameters is dictated by parameter uncertainty, performance sensitivity and identifiability. These will be discussed in the next section. A weighted nonlinear least squares approach is chosen to estimate the parameters. As opposed to the extended Kalman filter (Speetjens, 2009) there is no need for locally linearizing the system dynamics and making assumptions on noise levels of states and parameters. On the other hand nonlinear least squares is less efficient computationally. For the greenhouse parameters, which are part of the fast dynamics, we selected an update rate of 24 h, leaving ample time to perform nonlinear least squares in real-time. The update rate of 24 h is an order of magnitude smaller than the one used for control of the greenhouse dynamics in the inner loop, which is 0.5 h (Section 3.3). This is common practice in adaptive controller design to prevent instability.

Table 1
Bounds on greenhouse state variables.

State variable	X_c	X_T	$X_h/X_{h,sat}(X_T)$
Upper bound	2.75e−3	40.0	0.9
Lower bound	0	6.5	0

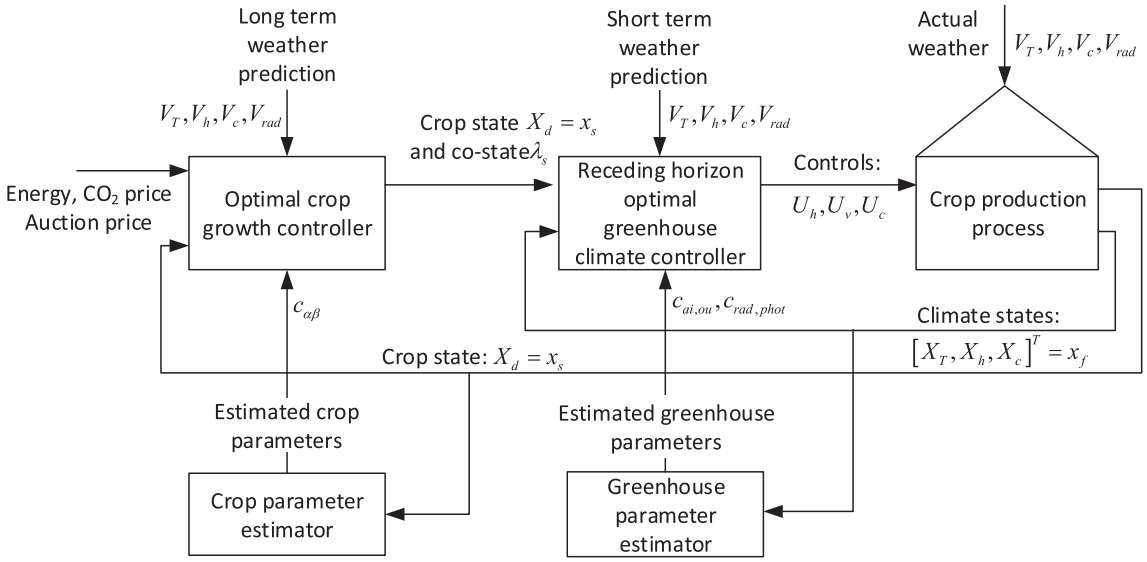

Fig. 1. Adaptive two time-scale receding horizon optimal control.

3. Results and discussion

3.1. Selection of model parameters for on-line adaptation

3.1.1. Introduction

Investigating possible benefits of adding on-line parameter estimation, i.e. the two blocks at the bottom of Fig. 1, to the two-time scale receding horizon controller represented by the remaining part of Fig. 1, is a major objective of this paper. To maximize possible benefits the estimated parameters should be selected sensibly. Parameter uncertainty and variability together with performance sensitivity and parameter identifiability guide a sensible choice of estimated parameters. Based on the performance sensitivity analysis of van Henten (2003) and prior knowledge about parameter values, variability and accuracy, $c_{\alpha\beta}$, $c_{rad,phot}$ and $c_{ai,ou}$ are selected as candidates.

3.1.2. Identifiability of $c_{\alpha\beta}$, $c_{rad,phot}$, and $c_{ai,ou}$ from different measurements

Using a recently developed, highly efficient algorithm (Stigter and Molenaar, 2015) we first investigate the identifiability of combinations of these parameters against different measured outputs being some or all of the states. If the singular values of the sensitivity matrix computed by the algorithm are all non-zero identifiability holds. Because the algorithm is of a numerical nature non-zero may mean “very small” i.e. showing a clear gap between the non-zero and these “very small” singular values.

If identifiability does not hold, null spaces corresponding to zero singular values, also obtained from a singular value decomposition of the sensitivity matrix computed by the algorithm, indicate linear combinations of parameters that cannot be identified because they are correlated.

Interestingly, from Table 2 observe that $c_{\alpha\beta}$, $c_{rad,phot}$, and $c_{ai,ou}$ are only simultaneously identifiable from crop dry weight measurements $y = X_d$. But crop dry weight is difficult to measure and represents the slow crop dynamics. Because $c_{rad,phot}$ and $c_{ai,ou}$ are parameters determining the fast greenhouse dynamics they need to be updated on that time-scale. So although identifiable in principal, in practice crop dry weight measurements cannot be used to estimate $c_{rad,phot}$ and $c_{ai,ou}$. Also observe from Table 2 that measuring any combination of states X_c, X_T, and X_h making up the fast greenhouse dynamics fails in identifying $c_{\alpha\beta}$, $c_{rad,phot}$, and $c_{ai,ou}$ simultaneously. The null space associated with the zero singular value for $y = X_c$, $y = \begin{bmatrix} X_c \\ X_T \end{bmatrix}$, as well as $y = \begin{bmatrix} X_c \\ X_T \\ X_h \end{bmatrix}$ has only a non-zero component for $c_{\alpha\beta}$, meaning that $c_{\alpha\beta}$ is not identifiable but $c_{rad,phot}$ and $c_{ai,ou}$ are simultaneously identifiable. For other combinations one null space has two non-zero components for $c_{\alpha\beta}$ and $c_{rad,phot}$. This means that only $c_{ai,ou}$ is identifiable. To summarize, identifying simultaneously $c_{rad,phot}$ and $c_{ai,ou}$ of the fast greenhouse dynamics is possible from $y = X_c$, $y = \begin{bmatrix} X_c \\ X_T \end{bmatrix}$, as well as $y = \begin{bmatrix} X_c \\ X_T \\ X_h \end{bmatrix}$. If one wants to identify $c_{\alpha\beta}$ this requires $y = X_d$. Although in theory $y = X_d$ is suitable to identify $c_{\alpha\beta}$, $c_{rad,phot}$, and $c_{ai,ou}$ simultaneously, due to the two time-scales it is not in practice. Because measurement of states X_c, X_T, and X_h are common in greenhouses we chose $y = \begin{bmatrix} X_c \\ X_T \\ X_h \end{bmatrix}$ to estimate $c_{rad,phot}$ and $c_{ai,ou}$.

3.2. Optimal control of crop growth

Two time-scale optimal control of crop growth according to Fig. 1 requires a long term slowly varying weather prediction for the entire growing period as well as prices for heating energy, CO_2 supply and selling harvested crops. These are again taken from van Henten (2003) apart from the weather prediction that is based on hourly recorded

Table 2
Singular values determining simultaneous identifiability of $c_{\alpha\beta}$, $c_{rad,phot}$ and $c_{ai,ou}$.

Measured outputs	$y = X_c$	$y = X_T$	$y = X_h$	$y = X_d$	$y = \begin{bmatrix} X_c \\ X_T \end{bmatrix}$	$y = \begin{bmatrix} X_T \\ X_h \end{bmatrix}$	$y = \begin{bmatrix} X_c \\ X_T \\ X_h \end{bmatrix}$
Singular values	8.15e−2	2.10	1.16	4.44e−1	2.10	2.40	2.40
	0.61e−2	0	0	1.88e−1	8.07e−2	0	8.07e−2
	0	0	0	5.99e−4	0	0	0

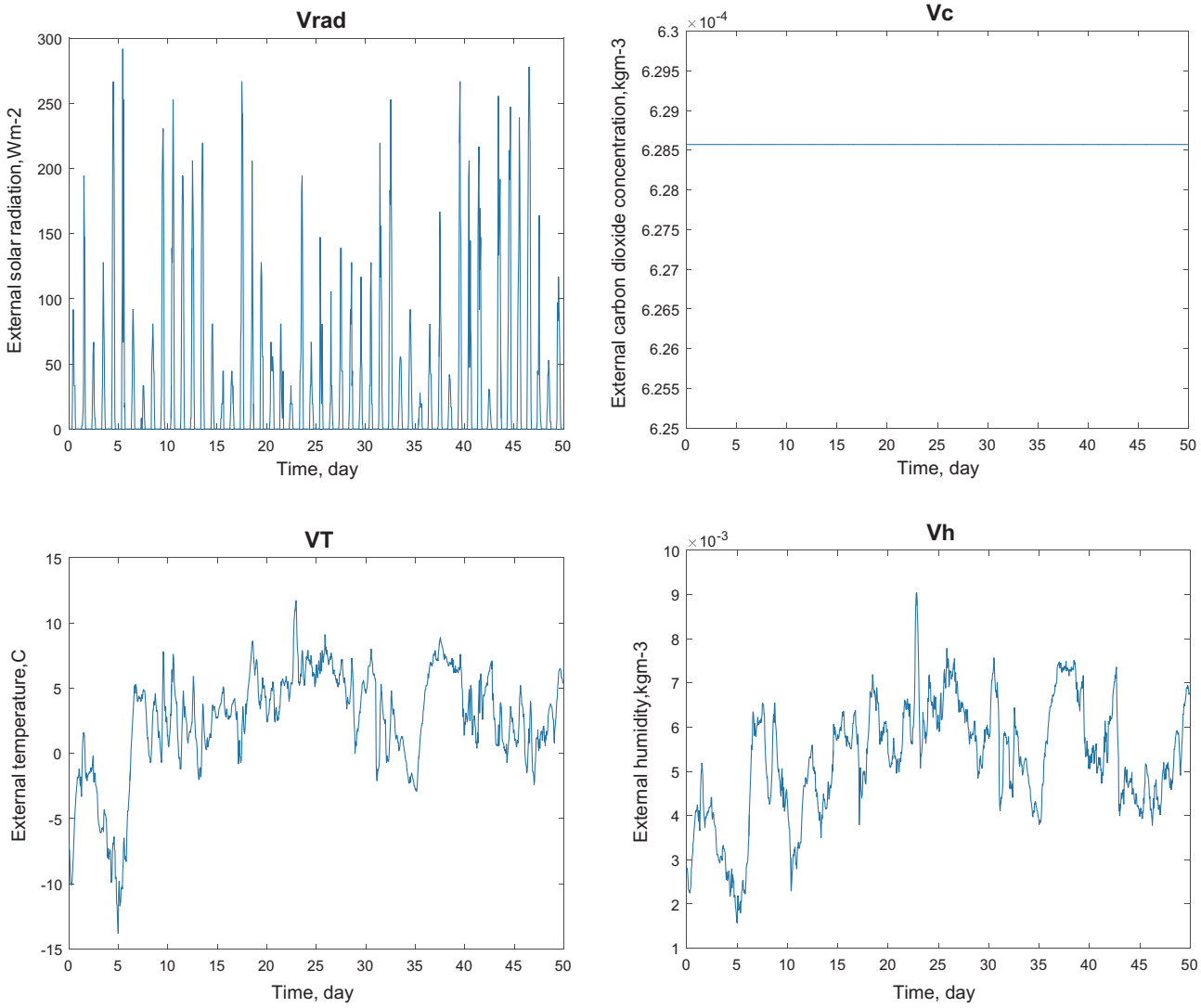

Fig. 2. External weather data over the entire growing season of 50 days.

weather data from the Netherlands that provides V_T, V_h, and V_{rad} (Breuer and van de Braak, 1989). For V_c we assumed a fixed value. These data are depicted in Fig. 2.

The optimal control computations in both the inner and outer loop of Fig. 1 are performed using Matlab optimal control software called PROPT (Rutquist and Edvall, 2010) which is part of Tomlab, a series of Matlab Toolboxes facilitating a large variety of optimizations performed by specialized software. Optimal control computations performed by PROPT are indeed "lightning fast" as advertised. They rely on polynomial approximations of functions and pseudospectral collocation transforming the problem into a nonlinear programming problem (Ross and Fahroo, 2004) that is solved very efficiently. The optimal control computation in the outer loop considers the greenhouse dynamics to be static. This comes down to setting to zero the state derivatives in Eqs. (2)–(4) as mentioned in Section 2.3. Our analysis, presented in the Appendix A, reveals that X_c is found from solving a quadratic equation in X_c for which the closed form solution is well known, although not necessarily unique. In our application only real solutions occurred of which we took the largest which most of the time appeared to be correct when compared to the true dynamic behaviour. States X_T and X_h can be directly expressed as a function of control and weather inputs. The bounds on X_c, X_T, and X_h, given by Table 1, thus turn into more complicated but directly computable constraints on the control inputs. Notice that crop dry weight X_d is the only state that remains, while the number of control inputs still equals three. These should be selected so as to satisfy the constraints we just mentioned while at the same time minimizing cost function (20).

To obtain a solution from the Matlab optimal control software PROPT we had to scale X_c, X_T, and X_h, which are quasi steady states, as well as state X_d and also all three controls U_c, U_q, and U_v such that their maximum values all become in the order of one. Also the final time was scaled to one. Although PROPT offers an auto-scaling option, it did not solve our problem. Moreover we had to recompute the solution several times while increasing the number of collocation points used by the algorithm up to 600, to finally obtain a solution with sufficient accuracy. Collocation points are time points where the polynomial approximations have to satisfy exactly conditions related to the optimal control problem and its solution (Rutquist and Edvall, 2010; Ross and Fahroo, 2004). As to the smoothed weather data, required by the optimal control computation, see Fig. 1, we simply took twelve samples from the hourly recorded weather data each day (so one each two hours) making the total number of samples equal to the number of collocation points.

The optimal state and corresponding co-state are shown in Fig. 3. Notice from Fig. 1, that the co-state is required for the receding horizon optimal controller in the inner loop, that controls the greenhouse

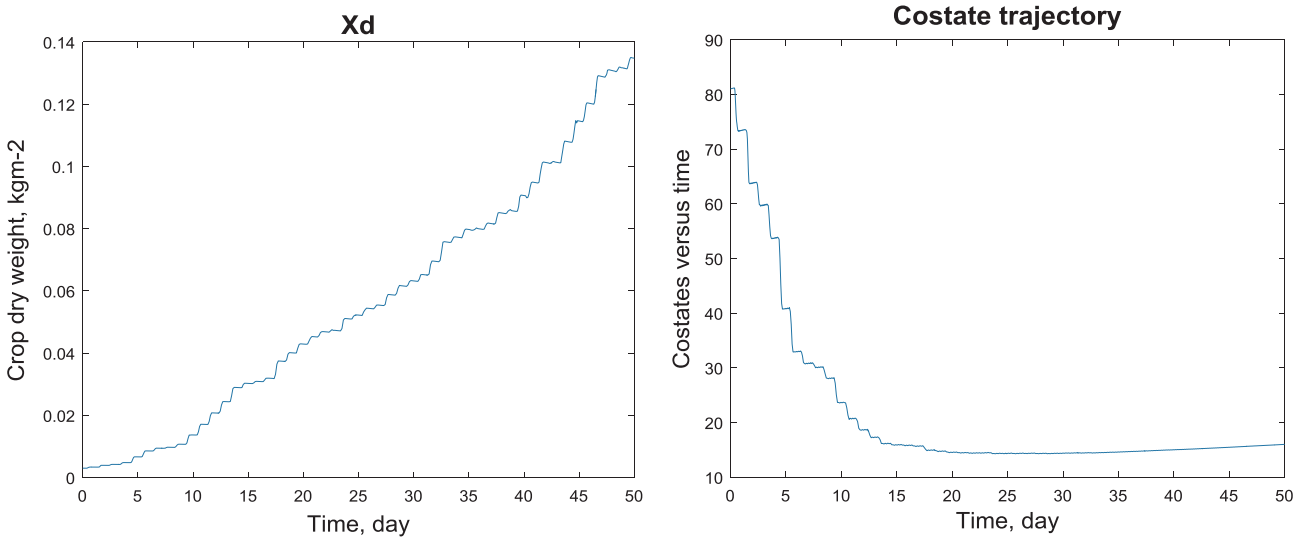

Fig. 3. Optimal slow state and co-state trajectory.

dynamics. Because PROPT uses polynomials, the co-state is not necessarily computed as it is for other types of optimal control algorithms. But fortunately, by making an additional call to a suitable function, PROPT can also produce the co-state trajectory.

To partly judge the outcome represented by Fig. 3, it may be compared with a similar optimal control computation performed by van Henten and Bontsema (2009). Comparing our Fig. 3 with their Fig. 1 reveals that the outcomes are very similar. Differences are mainly caused by different weather conditions.

3.3. Receding horizon optimal control of greenhouse climate

The inner loop of the adaptive two time-scale optimal controller in Fig. 1 is a receding horizon optimal controller (RHOC). It controls the fast dynamics (18) corresponding to the greenhouse climate, represented by states X_c, X_T, and X_h in Eqs. (2)–(4). The RHOC is an on-line digital optimal controller with a sampling period of 0.5 h and a control horizon of 3 h as mentioned in Section 2.3. Using the latest measurements of states X_c, X_T, and X_h to compute the initial state at the next 0.5 h, the receding horizon controller computes a digital piecewise constant optimal control over a horizon of 3 h starting from the next 0.5 h. After finishing this computation it sends the constant controls computed for the first 0.5 h at the next 0.5 h. The cost function used by the RHOC, denoted by J_{RHOC}, is given by,

$$J_{RHOC} = \int_{t_0}^{tf} (c_q U_q(t) + c_{CO_2} U_c(t)) - \lambda_s^T f_s(x_s, x_f, u) dt \tag{22}$$

The cost function in Eq. (22) contains the slow crop state $x_s = X_d$ as represented by Fig. 3 on the left as well as the "slow" co-state, denoted by λ_s as represented by Fig. 3 on the right. Both are obtained from the optimal control computation in the outer loop, as can be seen from Fig. 1. Both x_s and λ_s must be stored in the RHOC controller memory. The algorithm to compute digital optimal piecewise constant controls is described in van Straten et al. (2010). To speed up convergence of this algorithm it is initialized with a solution of the same optimal control problem found using PROPT again. The continuous time optimal control found by PROPT is averaged over each sampling period of 0.5 h providing a piecewise constant control that is close to optimal. This piecewise constant control initializes the digital optimal control computation. In this manner, on average, the digital optimal control computation finishes within 3 min and thus allows for real-time implementation given the sampling period of 0.5 h.

3.4. Adding on-line parameter estimation to the RHOC

3.4.1. Introduction

Based on arguments and identification results presented in Section 3.1 the possible benefit of on-line parameter estimation of $c_{\alpha,\beta}$, $c_{rad,phot}$, and $c_{ai,ou}$ is investigated. Because the weather, that acts as an external input, behaves partly periodic with a period of one day, we chose to update the greenhouse parameters $c_{rad,phot}$ and $c_{ai,ou}$ at the end of each day. Only if the outer loop optimal control computation is repeated, at several stages during the growing season, crop model parameter $c_{\alpha\beta}$ can be updated. To investigate the possible gain of on-line parameter estimation of $c_{rad,phot}$ and $c_{ai,ou}$ in Sections 3.4.2–3.4.4 we first compute performance sensitivities to these parameters and associated performance degradation due to errors in these parameters. These computation are performed with control being open-loop as well as closed-loop. Closed-loop control is realized by the RHOC in Fig. 1. Finally, in Section 3.4.4, benefits obtained from adding parameter estimation are investigated.

3.4.2. Performance sensitivity analysis of open-loop optimal control

For different values of parameters $c_{rad,phot}$ and $c_{ai,ou}$ Tables 3 and 4 present the maximum profit P obtained from optimal controls computed in the manner described in Section 3.3. These computations provide open-loop continuous-time optimal controls while using a static approximation of the greenhouse dynamics. In Table 3, $c_{rad,phot} = 3.55e{-}9$ is considered to be the actual parameter value denoted by $c^*_{rad,phot}$. This parameter value is taken as a reference. The corresponding value of P is denoted by P^*. The percentages in between brackets indicate relative changes from these reference values. Finally a relative sensitivity measure,

$$S = \frac{P - P^*}{c_{rad,phot} - c^*_{rad,phot}} \frac{c^*_{rad,phot}}{P^*} \tag{23}$$

Table 3
Performance and performance sensitivities associated with $c_{rad,phot}$.

$c_{rad,phot}$	P	S
3e−9 (−15.4930%)	2.8206 (−10.9210%)	0.7049
3.3e−9 (−7.0432%)	3.0043 (−5.1173%)	0.7267
$c^*_{rad,phot}$ = 3.55e−9	P^* = 3.1664	–
3.8e−9 (+7.0432%)	3.3192 (+4.8275%)	0.6855
4e−9 (+12.6761%)	3.4447 (+8.7905%)	0.6935

Table 4
Performance and performance sensitivities associated with $c_{ai,ou}$.

$c_{ai,ou}$	P	S
5.5 (−9.8361%)	3.2442 (+2.4591%)	−0.2500
5.8 (−4.9180%)	3.2033 (+1.1666%)	−0.2372
$c^*_{ai,ou}$ = 6.1	P^* = 3.1664	–
6.3 (+3.2787%)	3.1354 (−0.9794%)	−0.2987
6.5 (+6.5574%)	3.1190 (−1.4974%)	−0.2284

is shown in Tables 3 and 4 that approximates the relative sensitivity measure

$$\left.\frac{\partial P}{\partial c_{rad,phot}}\frac{c_{rad,phot}}{P}\right|_{c^*_{rad,phot}} \tag{24}$$

Table 4 is similar to Table 3 with $c_{rad,phot}$ replaced by $c_{ai,ou}$.

We may compare the relative sensitivity measure S to results found from the first-order sensitivity analysis performed by van Henten (2003). He found 1.1783 and −0.3418 to be the relative performance sensitivities to $c_{rad,phot}$ and $c_{ai,ou}$ respectively. Because S is only an approximation of the first-order sensitivity this partly explains the difference. The main difference however is due to differences with weather conditions used by van Henten (2003).

3.4.3. Performance sensitivity analysis of closed-loop optimal control

Instead of open-loop control, closed-loop control is applied to counteract errors such as modelling errors and errors in weather predictions. In this section, by means of simulations, the sensitivity to errors in model parameters $c_{rad,phot}$ and $c_{ai,ou}$ is investigated when closed-loop control is applied. This situation is represented by Fig. 1 when the dynamics of the crop production system together with its initial state and external inputs are identical to the ones used to compute the optimal controls in both the inner and outer loop, except for the parameter values of $c_{rad,phot}$ and $c_{ai,ou}$. The crop production system has fixed parameter values $c_{rad,phot} = c^*_{rad,phot} = 3.55e{-}9$ and $c_{ai,ou} = c^*_{ai,ou} = 6.1$ as given in Tables 3 and 4. Different values of parameters $c_{rad,phot}$ and $c_{ai,ou}$ used to compute the optimal control in both the inner and outer loop and the corresponding performance P_C of the crop production system are listed in Tables 5 and 6 respectively. Also the optimal performance P, as obtained from the initial optimal control computation with the erroneous parameter value, is listed. In Table 5, as before, sensitivity measure S is given by Eq. (23). Sensitivity measure S_C is given by Eq. (23) with P replaced with P_C. Similar arguments apply to Table 6 with parameter $c_{rad,phot}$ replaced with $c_{ai,ou}$ in Eq. (23).

When judging the overall performance P_C of the crop production system by means of Tables 5 and 6 we must not forget the fact that the optimal control problem has state constraints. When erroneous parameter values are used to compute the optimal control, these state constraints may be violated by the crop production system. Therefore Tables 5 and 6 also show a measure C_X of constraint violation. As can be seen from Tables 5 and 6, in some cases of erroneous parameter values, the violation of constraints is accompanied with improvement of performance. This may appear counterintuitive but is not when one realizes that satisfying state constraints takes preference over optimizing performance. Also observe that when the parameter values are without error, i.e. when $c_{rad,phot} = c^*_{rad,phot} = 3.55e{-}9$ and $c_{ai,ou} = c^*_{ai,ou} = 6.1$ constraints are violated slightly because $C_X = 0.1189e{-}3 > 0$. This is due to technicalities of the optimal control algorithm which satisfies state constraints at a limited number of time points only (van Straten et al., 2010). Therefore values of C_X above $0.1189e-3$ should be interpreted as violating constraints while values below should be interpreted as satisfying constraints.

When comparing the outcomes of P with P_C in Tables 5 and 6, an important conclusion is that the influence of erroneous parameter values on P_C is much reduced as compared to P, especially for $c_{rad,phot}$. Recall that P is obtained from the initial optimal control computation which is essentially open-loop. The reduced influence of parameter errors on P_C, the actual performance of the crop production system, is clearly the result of closed-loop instead of open-loop control. This confirms the major objective of closed-loop control which is to counteract errors. Another important observation obtained by comparing P with P_C is that parameter errors cause significant differences between them. These differences $P{-}P_C$ represent the error of model predictions of the optimal performance. Accurate estimates of optimal performance are crucial for decisions on investments. Therefore these errors and associated sensitivities are recorded in Tables 7 and 8. The percentage listed in between brackets in the $P{-}P_C$ columns represents the fraction $(P{-}P_C)/P_C$. Furthermore in Table 7,

$$S_e = \frac{P-P_C}{c_{rad,phot}-c^*_{rad,phot}}\frac{c^*_{rad,phot}}{P_C} \tag{25}$$

which approximates the relative sensitivity of errors of optimal performance estimates for errors in parameter $c_{rad,phot}$. Eq. (25) also applies to Table 8 when $c_{rad,phot}$ is replaced with $c_{ai,ou}$.

From Tables 7 and 8 observe that the accuracy of optimal performance estimates is especially sensitive to parameter errors in $c_{rad,phot}$.

By adding parameter adaptation, i.e. the two lower blocks in Fig. 1, to the control scheme represented by the rest of Fig. 1, the errors investigated and quantified in this section may be reduced. If perfect parameter estimates are obtained, they are removed. The possible reduction or removal will be investigated in the next section.

3.4.4. Performance and improvements associated with adaptive control

On-line parameter estimation of $c_{rad,phot}$ and $c_{ai,ou}$ is performed in the inner loop of Fig. 1, as represented by the lower right block. The outer loop optimal control computation is assumed to be performed only once, at the start of the growing season. This excludes use of the lower left block in Fig. 1. Given the simultaneous identifiability of $c_{rad,phot}$ and $c_{ai,ou}$ from X_c, X_T, and X_h established in Section 3.1.2, we expect accurate on-line parameter estimates when no measurement and modelling errors are assumed to be present and when perfect short term weather predictions are available. By means of simulations of the control system represented by Fig. 1, i.e. including the on-line parameter estimation represented by the lower right block, we established that almost perfect on-line parameter estimates (within 0.1% of the true value) are obtained of $c_{rad,phot}$ and $c_{ai,ou}$. This is already achieved after the first parameter update. Parameter updates are performed at 0.00 a.m. each day using measurements of states X_c, X_T, and X_h as well as the weather of only the previous day. The sampling interval is 0.5 h. Given

Table 5
Performance and performance sensitivities associated with $c_{rad,phot}$.

$c_{rad,phot}$	P	S	P_C	S_C	C_X
3e−9 (−15.4930%)	2.7692 (−10.9043%)	0.7038	3.0868 (−0.6886%)	0.0444	0.3829e−4
3.3e−9 (−7.0432%)	2.9566 (−4.8764%)	0.6924	3.1013 (−0.2210%)	0.0314	0.5030e−4
$c^*_{rad,phot}$ = 3.55e−9	P^* = 3.1082	–	P^* = 3.1082	–	0.1189e−3
3.8e−9 (+7.0432%)	3.2571 (+4.7909%)	0.6803	3.1125 (+0.1385%)	0.0197	0.3590e−3
4e−9 (+12.6761%)	3.3740 (+8.5520%)	0.6747	3.1146 (+0.2061%)	0.0163	0.5837e−3

Table 6
Performance and performance sensitivities associated with $c_{ai,ou}$.

$c_{ai,ou}$	P	S	P_C	S_C	C_X
5.5 (−9.8361%)	3.1412 (+1.0631%)	−0.1081	3.1250 (+0.5419%)	−0.0551	0.3373e−2
5.8 (−4.9180%)	3.1256 (+0.5604%)	−0.1139	3.1171 (+0.2886%)	−0.0587	0.1765e−2
$c^*_{ai,ou}$ = 6.1	P^* = 3.1082	–	P^* = 3.1082	–	0.1189e−3
6.3 (+3.2787%)	3.0970 (−0.3600%)	−0.1098	3.1030 (−0.1671%)	−0.0510	0.1143e−3
6.5 (+6.5574%)	3.0848 (−0.7521%)	−0.1147	3.0970 (−0.3582%)	−0.0546	0.1114e−3

Table 7
Performance estimate errors and their sensitivity for parameter errors in $c_{rad,phot}$.

$c_{rad,phot}$	$P-P_C$	S_e
3 (−15.4930%)	−0.3176 (−10.2890%)	0.6641
3.3 (−7.0432%)	−0.1447 (−4.6658%)	0.6624
$c^*_{rad,phot}$ = 3.55e−9	$P^*-P^*_C$ = 0	–
3.8 (+7.0432%)	0.1446 (+4.6458%)	0.6596
4 (+12.6761%)	0.2594 (+8.3285%)	0.6570

Table 8
Performance estimate errors and their sensitivity for parameter errors in $c_{ai,ou}$.

$c_{ai,ou}$	$P-P_C$	S_e
5.5 (−9.8361%)	0.0162 (+0.5184%)	−0.0527
5.8 (−4.9180%)	0.0085 (+0.2727%)	−0.0554
$c^*_{ai,ou}$ = 6.1	$P^*-P^*_C$ = 0	–
6.3 (+3.2787%)	−0.0060 (−0.1934%)	−0.0590
6.5 (+6.5574%)	−0.0122 (−0.3939%)	−0.0601

Table 9
Measurement accuracy of climate states and external weather.

Measurement	V_{rad}	V_C	V_T	V_h	X_c	X_T	X_h
Accuracy	5%	3%	0.5 °C	4.5%	3%	0.5 °C	4.5%

the high accuracy of parameter estimates the errors mentioned in the previous section disappear almost completely.

Since one of the objectives of the RHOC in the inner loop of Fig. 1 is to counteract measurement errors we added random uniformly distributed measurement errors on the greenhouse climate states X_c, X_T, and X_h as well external weather inputs V_{rad}, V_C, V_T, and V_h. The magnitude of these errors were chosen to match absolute and relative accuracies obtained from several data sheets from common sensors to measure these variables. They are listed in Table 9.

Table 10
Performance of the characteristic run.

Parameter	P	P_C	$\left\lvert\frac{c-c^*}{c^*}\right\rvert$	$\left\lvert\frac{P-P_C}{P_C}\right\rvert$	C_X
$c_{rad,phot}$	3.1123	3.1077	0.7043%	0.1504%	0.7414e−3
$c_{ai,ou}$	3.1081	3.1076	0.8668%	0.0179%	0.7384e−3

Fig. 4 shows a characteristic run of the adaptive RHOC in Fig. 1. The estimates of $c_{rad,phot}$ are within 3.3e−9 and 3.8e−9. These two values are recorded in Tables 3, 5 and 7. The associated errors can thus be directly read from those tables. They represent a worst case of the error remaining after introducing on-line parameter adaptation, since most of the time the parameter error is much smaller, as seen from Fig. 4. Similar arguments hold for $c_{ai,ou}$ the estimates of which stay within 5.8 and 6.3 two values recorded in Tables 4, 6 and 8. Exact values of the time-averaged absolute error of both parameter estimates, denoted by $\left\lvert\frac{c-c^*}{c^*}\right\rvert$, and the associated relative performance loss $\left\lvert\frac{P-P_C}{P_C}\right\rvert$ of the characteristic run are given in Table 10.

$c_{rad,phot}$ represents light use efficiency. It is possible that as time goes by, light use efficiency might decrease because of accumulation of stains. $c_{ai,ou}$ represents the heat transmission coefficient through the greenhouse cover. It is also possible that the heat transmission coefficient increases with degradation of the greenhouse cover material. So both parameters are likely to be time-varying. This is another good reason to introduce adaptive control, which adapts parameters as they change. Assume $c^*_{rad,phot}$ starts from 3.8e−9, and decreases by 0.1e−9 every day. And, after cleaning every week, $c^*_{rad,phot}$ goes back to 3.8e−9. Also assume $c^*_{ai,ou}$ starts from 5.8, and increases by 0.01 every day. Fig. 5 represents a characteristic run showing the tracking capabilities of on-

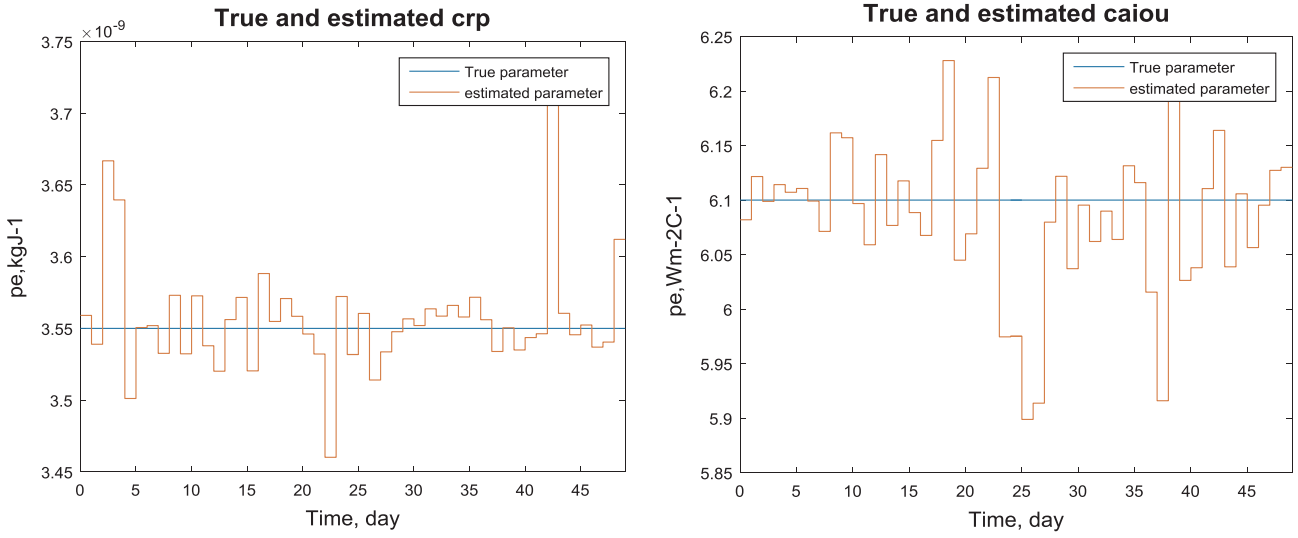

Fig. 4. Estimated $c_{rad,phot}$ and $c_{ai,ou}$ from a characteristic run of the adaptive RHOC.

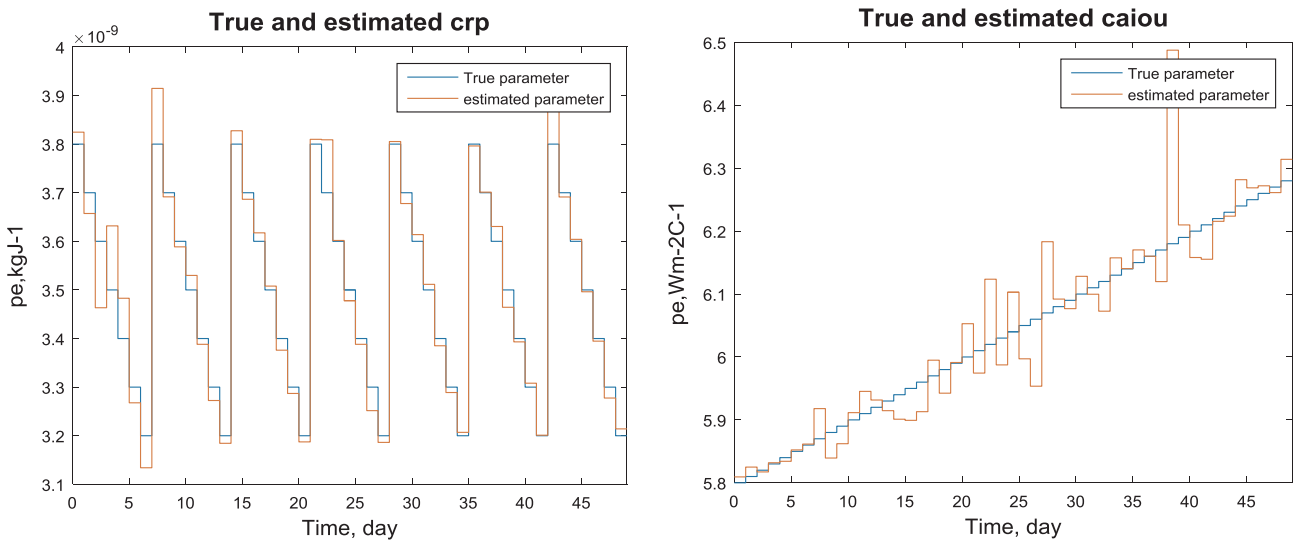

Fig. 5. Estimates of time-varying $c_{rad,phot}$ and $c_{ai,ou}$ from a characteristic run of the adaptive RHOC.

line parameter estimates if $c^*_{rad,phot}$ and $c^*_{ai,ou}$ vary each day. Their accuracy appears similar to when $c^*_{rad,phot}$ and $c^*_{ai,ou}$ are constant implying very good tracking capability.

4. Conclusions

Adding on-line parameter estimation to a two time-scale receding horizon optimal controller for lettuce crop production in greenhouses improves performance of the crop production system. The improvement especially concerns constraint violations that are reduced by a factor 5 to 30. The improvement of profit turned out very small, namely less than 1%. This may seem surprising but can be explained in two different ways. Firstly, the effect on performance of parameter errors, usually computed and reported in the literature, does not incorporate any feedback mechanism, i.e. a mechanism *counteracting* (parameter) errors. A two time-scale receding horizon controller does, and apparently is *very successful* in eliminating parameter errors, at least in the case considered in this paper. This is confirmed by the *open-loop* control computations performed in this paper. They lack a feedback mechanism and reveal performance improvements just over 10%. Secondly, the state constraints actually represent the limited range of the crop model. Outside this range the crop model produces too optimistic growth and ignores other phenomena like diseases. Therefore in actual practice, improvement of constraint satisfaction comes down to improving profit.

A-priori estimates of optimal performance rely on *open-loop* control and are crucial as it comes to decisions on investments. So for *a priori* performance estimates the possible accuracy improvement computed in this paper is just over 10%. However, this improvement requires *a priori* known parameter estimates. These can only be obtained from data obtained in previous growing seasons. They do not require on-line parameter adjustment but are obtained from *off-line* parameter estimation.

The three candidate parameters for on-line adjustment in this paper turned out to be identifiable from just a single measurement, being the state variable representing crop dry weight. But this paper also revealed that, due to the two time-scale decomposition, estimating all three candidate parameters *on-line*, using only crop dry weight measurement, is not feasible in Fig. 1. Measurement of all three greenhouse climate states, failed to identify all three candidate parameters, but allowed to identify only the two that relate to greenhouse climate. These two parameters could even be identified from a single measurement being the state representing CO_2 concentration in the greenhouse. Finally, from measurement of all three greenhouse climate states, these two candidate parameters can be estimated on-line in Fig. 1, with an accuracy of ± 5%, even if they vary slowly over time. The associated optimal control computations as well as the *on-line* parameter estimation can be performed in real-time if a sampling interval of 0.5 h is used.

Acknowledgements

The discussions with Eldert van Henten, Karel Keesman, Bert van Ooster and Rachel van Ooteghem have largely contributed to the ripening of ideas in this paper. This work was financially supported by the China Scholarship Council – China (201506350209).

Appendix A. Quasi steady state computation

Explicit expressions for quasi steady-states X_T, X_h, and X_c are derived below in terms of X_d as well as controls U_c, U_q, U_v and weather inputs V_{rad}, V_T, V_c, V_h.

Quasi steady state X_T notations, equations and computations:

$$U_q - \underbrace{(c_{cap,q,v}U_v + c_{ai,ou})}_{f_1}(X_T - V_T) + \underbrace{c_{rad,q}V_{rad}}_{f_2} = 0 \tag{A1}$$

$$U_q - f_1(X_T - V_T) + f_2 = 0 \tag{A2}$$

$$f_1 X_T = U_q + f_1 V_T + f_2 \tag{A3}$$

$$X_T = \frac{U_q + f_1 V_T + f_2}{f_1} \tag{A4}$$

$\dot{X}_T$ is set to zero as in Eq. (A1). X_T is then found from Eq. (A4).

Quasi steady state X_h notations:

$$\varphi_{vent,h} = \underbrace{(U_v + c_{leak})}_{U_{vcl}}(X_h - V_h) = U_{vcl}(X_h - V_h) \tag{A5}$$

$$\varphi_{transp,h} = \underbrace{c_{Xd}c_{v,pl,ai}}_{f_3}\left(\underbrace{\frac{c_{v,1}}{c_R(X_T + c_{T,abs})}e^{c_{v,2}X_T/(X_T+c_{v,3})}}_{f_4} - X_h\right) = f_3(f_4 - X_h) \tag{A6}$$

Quasi steady state X_h equations and computations:

$$\varphi_{transp,h} - \varphi_{vent,h} = 0 \tag{A7}$$

$$f_3(f_4 - X_h) - U_{vcl}(X_h - V_h) = 0 \tag{A8}$$

$$f_3 f_4 - f_3 X_h - U_{vcl}X_h + U_{vcl}V_h = 0 \tag{A9}$$

$$(f_3 + U_{vcl})X_h = f_3 f_4 + U_{vcl}V_h \tag{A10}$$

$$X_h = \frac{f_3 f_4 + U_{vcl}V_h}{f_3 + U_{vcl}} \tag{A11}$$

$\dot{X}_h$ is set to zero as in Eq. (A7). X_h is then found from Eq. (A11) with X_T given by Eq. (A4).

Quasi steady state X_c notations:

$$\varphi_{phot,c} = \underbrace{(1 - e^{c_{pl,d}X_d})}_{c_{Xd}}\frac{c_{rad,phot}V_{rad}(-c_{CO2,1}X_T^2 + c_{CO2,2}X_T - c_{CO2,3})(X_C - c_\Gamma)}{\underbrace{c_{rad,phot}V_{rad}}_{c_{Vr}} + \underbrace{(-c_{CO2,1}X_T^2 + c_{CO2,2}X_T - c_{CO2,3})}_{c_T}(X_C - c_\Gamma)} \tag{A12}$$

$$\varphi_{phot,c} = \frac{c_{Xd}c_{Vr}c_T(X_C - c_\Gamma)}{c_{Vr} + c_T(X_C - c_\Gamma)} \tag{A13}$$

$$\varphi_{vent,c} = \underbrace{(U_v + c_{leak})}_{U_{vcl}}(X_c - V_c) = U_{vcl}(X_c - V_c) \tag{A14}$$

$$c_{DU} = c_{resp,c}X_d 2^{(0.1X_T - 2.5)} + U_c \tag{A15}$$

Quasi steady state X_c equations and computations:

$$\varphi_{phot,c} + \varphi_{vent,c}\underbrace{-c_{resp,c}X_d 2^{(0.1X_T - 2.5)} - U_c}_{-c_{DU}} = 0 \tag{A16}$$

$$\frac{c_{Xd}c_{Vr}c_T(X_c - c_\Gamma)}{c_{Vr} + c_T(X_c - c_\Gamma)} + U_{vcl}(X_c - V_c) - c_{DU} = 0 \tag{A17}$$

$$c_{Xd}c_{Vr}c_T(X_c - c_\Gamma) + (U_{vcl}(X_c - V_c) - c_{DU})(c_{Vr} + c_T(X_c - c_\Gamma)) = 0 \tag{A18}$$

By setting $\dot{X}_c$ to zero as in Eq. (A16), X_c is found from Eq. (A18) which is a quadratic equation,

$$aX_c^2 + bX_c + c = 0 \tag{A19}$$

with,

$$a = U_{vcl}c_T \tag{A20}$$

$$b = c_{Xd}c_{Vr}c_T + U_{vcl}c_{Vr} - U_{vcl}c_T c_\Gamma - U_{vcl}V_c c_T - c_{DU}c_T \tag{A21}$$

$$c = -c_{Xd}c_{Vr}c_T c_\Gamma - U_{vcl}V_c c_{Vr} - U_{vcl}c_{DU}c_{Vr} + U_{vcl}V_c c_T c_\Gamma - c_{DU}c_{Vr} + c_{DU}c_T c_\Gamma \tag{A22}$$

References

Arvanitis, K.G., Paraskevopoulos, P.N., Vernardos, A.A., 2000. Multirate adaptive temperature control of greenhouses. Comput. Electron. Agric. 26 (3), 303–320.

Berenguel, M., Yebra, L.J., Rodríguez, F., 2003. Adaptive control strategies for greenhouse temperature control. ECC 2747–2752.

Breuer, J.J.G., van de Braak, N.J., 1989. Reference year for Dutch greenhouses. Acta Hortic. 248, 101–108.

Cunha, J.B., 2006. Real-time adaptive control for greenhouse heating, cooling and CO_2 enrichment. Proc. Comp. Agr. Nat. Res., 4th World Congr. Conf., Orlando., pp. 116–121.

Davis, P.F., 1984. A technique of adaptive control of the temperature in a greenhouse using ventilator adjustments. J. Agr. Eng. Res. 241–248.

Gonzalez, R., Rodriguez, F., Guzman, J.L., Berenguel, M., 2014. Robust constrained economic receding horizon control applied to the two time-scale dynamics problem of a greenhouse. Optim. Contr. Appl. Met. 35 (4), 435–453.

Hooper, A.W., Davis, P.F., 1985. Control of greenhouse air temperature with an adaptive control algorithm. Acta Hortic. 174, 407–412.

Ioslovich, I., Gutman, P.O., Seginer, I., 2004. Dominant parameter selection in the marginally identifiable case. Math. Comput. Simulat. 65 (1), 127–136.

Ioslovich, I., Gutman, P.O., Linker, R., 2009. Hamilton–Jacobi–Bellman formalism for optimal climate control of greenhouse crop. Automatica 45 (5), 1227–1231.

Kokotović, P.V., Khalil, H.K., O'reilly, J., 1986. Singular Perturbations in Control: Analysis and Design. Academic Press, London.

Rodríguez, F., Guzmán, J.L., Berenguel, M., Arahal, M.R., 2008. Adaptive hierarchical control of greenhouse crop production. Int. J. Adapt. Control. 22 (2), 180–197.

Ross, I.M., Fahroo, F., 2004. Pseudospectral knotting methods for solving nonsmooth optimal control problems. J. Guid. Control. Dynam. 27 (3), 397–405.

Rutquist, P.E., Edvall, M.M., 2010. Propt-Matlab Optimal Control Software. Tomlab optimization Inc.

Speetjens, S.L., 2008. Towards model based adaptive control for the Watergy greenhouse.

[PhD thesis]. Wageningen University, Wageningen, The Netherlands.
Speetjens, S.L., Stigter, J.D., van Straten, G., 2009. Towards an adaptive model for greenhouse control. Comput. Electron. Agric. 67 (1), 1–8.
Stigter, J.D., Molenaar, J., 2015. A fast algorithm to assess local structural identifiability. Automatica 58, 118–124.
Tap, F., 2000. Economics-based optimal control of greenhouse tomato crop production. [PhD thesis]. Wageningen University, Wageningen, The Netherlands.
Udink ten Cate, A.J., van de Vooren, J., 1978. Adaptive control of a glasshouse heating system. Acta Hortic. 76, 121–125.
Udink ten Cate, A.J., 1983. Modeling and (adaptive) control of greenhouse climates. [PhD thesis]. Wageningen University, Wageningen, The Netherlands.
van Beveren, P.J.M., Bontsema, J., van Straten, G., van Henten, E.J., 2015. Minimal heating and cooling in a modern rose greenhouse. Appl. Energ. 137, 97–109.
van Henten, E.J., 1994. Greenhouse climate management: an optimal control approach. [PhD thesis]. Wageningen University, Wageningen, The Netherlands.
van Henten, E.J., 2003. Sensitivity analysis of an optimal control problem in greenhouse climate management. Biosyst. Eng. 85 (3), 355–364.
van Henten, E.J., Bontsema, J., 2009. Time-scale decomposition of an optimal control problem in greenhouse climate management. Control. Eng. Pract. 17 (1), 88–96.
van Ooteghem, R.J.C., 2007. Optimal control design for a solar greenhouse. [PhD thesis]. Wageningen University, Wageningen, The Netherlands.
van Straten, G., Challa, H., Buwalda, F., 2000. Towards user accepted optimal control of greenhouse climate. Comput. Electron. Agric. 26 (3), 221–238.
van Straten, G., van Willigenburg, G., van Henten, E., van Ooteghem, R., 2010. Optimal Control of Greenhouse Cultivation. CRC Press, USA.
van Straten, G., 2013. Optimal greenhouse cultivation control: Quo vadis? IFAC Proc. Vol. 46 (4), 11–16.
van Willigenburg, L.G., van Henten, E.J., van Meurs, W.T.H.M., 2000. Three time-scale digital optimal receding horizon control of the climate in a greenhouse with a heat storage tank. IFAC Proc. Vol. 149–154.